SI-HEP-2005-07
SFB/CPP-05-27
hep-ph/0506269
February 2, 2008

Non-factorizable contributions to deep inelastic scattering at large x

Ben D. Pecjak
Theoretische Physik 1, Fachbereich Physik, Universität Siegen
D-57068 Siegen, Germany

Abstract

We use soft-collinear effective theory (SCET) to study the factorization properties of deep inelastic scattering in the region of phase space where $(1-x) \sim \Lambda_{\rm QCD}/Q$. By applying a regions analysis to loop diagrams in the Breit frame, we show that the appropriate version of SCET includes anti-hard-collinear, collinear, and soft-collinear fields. We find that the effects of the soft-collinear fields spoil perturbative factorization even at leading order in the $1/Q$ expansion.

1 Introduction

This paper deals with the factorization properties of deep inelastic scattering (DIS) in the region of phase space where $1-x \sim \Lambda_{\rm QCD}/Q$, with Q the large energy carried by the virtual photon. In this kinematical region the final-state jet carries an energy of order Q, but has a small invariant mass $p_x^2 = Q^2(1-x)/x \sim Q\Lambda_{\rm QCD}$. We assume that perturbation theory is valid at both the hard scale Q^2 and the jet scale $Q\Lambda_{\rm QCD}$. The invariant mass of the target proton defines a third, non-perturbative scale $M_P^2 \sim \Lambda_{\rm QCD}^2$. In similar cases in inclusive B decay it is possible to derive factorization formulas which separate the physics from the three scales $Q^2 \gg Q\Lambda_{\rm QCD} \gg \Lambda_{\rm QCD}^2$ into a convolution of the generic form [1]

$$H \cdot J \otimes S. \tag{1}$$

The functions H and J are perturbatively calculable hard and jet functions depending on fluctuations at the scales Q^2 and $Q\Lambda_{\rm QCD}$ respectively, and S is a non-perturbative function containing physics at the low-energy scale $\Lambda_{\rm QCD}^2$. The symbol $\otimes$ stands for a convolution. Our goal is to use effective field theory methods to establish whether such a factorization formula can be derived for deep inelastic scattering in the large-x limit.

Recent studies of perturbative factorization in B decay have relied heavily on soft-collinear effective theory (SCET) [2, 3, 4, 5]. These include many applications to inclusive decay, both at leading order [3, 6, 7] and including power corrections [8, 9, 10]. For inclusive B decay these proofs are rather straightforward. Inclusive decay deals with interactions between hard-collinear particles fluctuating at the jet scale $m_b\Lambda_{\rm QCD}$ with soft particles fluctuating at the non-perturbative scale $\Lambda_{\rm QCD}^2$. The leading-order Lagrangian interactions between soft and hard-collinear particles can be decoupled by field redefinitions involving Wilson lines [3]. After integrating out hard fluctuations in a first step of matching, the factorization of the SCET matrix elements into a convolution of jet and soft functions is more or less a natural consequence of this decoupling at the level of the Lagrangian.

Applications of SCET to exclusive decay are considerably more complicated [11, 12, 13, 14]. Exclusive processes typically involve both soft and collinear particles fluctuating at the scale $\Lambda_{\rm QCD}^2$, in addition to hard-collinear fluctuations which are integrated out in the first step of a two-step matching procedure. It has been argued that a low-energy theory of soft and collinear particles contains a third mode, referred to as soft-collinear [15]. This follows from an analysis of loop diagrams with soft and collinear external lines by the method of regions [16]. This soft-collinear "messenger mode" has the special property that it can interact with both soft and collinear particles without taking them far off shell. These modes introduce an additional, highly non-perturbative soft-collinear scale $\Lambda_{\rm QCD}^3/Q$. To prove factorization formulas of the type in (1), one must show that the effects of this fourth scale are irrelevant to the low-energy matrix elements defining the soft functions S. This has been emphasized in [14, 17, 18]. In B decay the soft-collinear scale is relevant at the endpoints of convolution integrals linking non-perturbative soft and collinear functions, so the soft-collinear field has often been associated with endpoint divergences in these integrals [14].

In this paper we show that the soft-collinear mode is relevant to an analysis of DIS at large x. Near the endpoint, DIS involves the three widely separated scales $Q^2 \gg (1-x)Q^2 \gg \Lambda_{\rm QCD}^2$. Our main finding is that we cannot correlate the two small scales by the definition $\lambda^2 \sim (1-x) \sim \Lambda_{\rm QCD}/Q$ without introducing a fourth scale, $\Lambda_{\rm QCD}^3/Q \sim Q^2\lambda^6$. The appearance of this fourth scale is associated with the soft-collinear mode. For values of x satisfying $1-x \sim \Lambda_{\rm QCD}/Q$, the low-energy matrix element defining the parton distribution function involves fluctuations at both the collinear and soft-collinear scales. An attempt to use effective field theory methods to prove a factorization formula such as (1) leads instead to an expression

$$H\left(\frac{Q^2}{\mu^2}\right) J\left(\frac{Q^2(1-x)}{\mu^2}, \frac{Q\omega_{sc}}{\mu^2}\right) \otimes f\left(\frac{\Lambda_{\rm QCD}^2}{\mu^2}, \frac{\Lambda_{\rm QCD}^2\omega_{sc}}{Q\mu^2}\right), \tag{2}$$

where $\omega_{sc} \sim \Lambda_{\rm QCD}$ is a convolution variable. Since the parton distribution function f contains a non-perturbative dependence on the large energy Q, factorization is spoiled.

The organization of this paper is as follows. In Section 2 we define our power counting and identify the relevant SCET fields by applying the method of regions to a representative loop diagram. Section 3 deals with matching the QCD Lagrangian and electromagnetic current onto a version of SCET which accounts for these momentum regions. In Section 4 we show with a tree-level example that the parton distribution function is sensitive to soft-collinear effects, and discuss this further in Section 5 with a one-loop calculation. In Section 6 we summarize the implications of the soft-collinear mode on factorization. We compare our results with previous work in Section 7 and conclude in Section 8.

2 Power counting and momentum regions

Deep inelastic scattering involves the scattering of an energetic virtual photon with a large invariant mass $q^2 = -Q^2$ off a proton with momentum P to form a hadronic jet carrying momentum p_x and an invariant mass $p_x^2 = Q^2(1-x)/x$, where

$$x = -\frac{q^2}{2P\cdot q} = \frac{Q^2}{2P\cdot q}. \tag{3}$$

We are interested in the region of phase space where the hadronic jet carries a large energy of order Q, but has a small invariant mass on the order of the jet scale $Q\Lambda_{\rm QCD}$. More precisely, we work in the kinematic region where $p_x^2 \sim Q\Lambda_{\rm QCD} \sim Q^2(1-x)$. This correlates the two small scales $1-x \sim \Lambda_{\rm QCD}/Q$. We make this explicit in the effective theory by introducing an expansion parameter $\lambda^2 \sim (1-x) \sim \Lambda_{\rm QCD}/Q$. We then calculate the cross section as a double series in the perturbative coupling constant and λ. In terms of λ the invariants $P\cdot p_x \sim Q^2$, $p_x^2 \sim Q^2\lambda^2$, and $P^2 \sim Q^2\lambda^4$ define three widely separated scales $Q^2 \gg Q^2\lambda^2 \gg Q^2\lambda^4$. In this paper we investigate whether we can derive a factorization formula which separates the physics from these scales.

Our analysis relies on soft-collinear effective theory. Unlike in applications of SCET to B decay, there is no natural Lorentz frame in which to describe the scattering process. We find the Breit frame most convenient for what follows. In terms of two light-like vectors $n_\pm$ satisfying $n_+n_- = 2$, the components of the photon momentum q^μ in the Breit frame are given by $(n_+q, q_\perp, n_-q) = (-Q, 0, Q)$. If the proton momentum is $P = (Q/x, 0, M_p^2 x/Q)$, then at leading order in λ the jet momentum $p_x = q + P$ is given by $p_x = (Q(1-x)/x, 0, Q)$ and satisfies $p_x^2 = Q^2(1-x)/x$. We will refer to momenta with the scaling $p_c \sim Q(1, \lambda^2, \lambda^4)$ as collinear, and momenta with the scaling $p_{\bar{hc}} \sim Q(\lambda^2, \lambda, 1)$ as anti-hard-collinear. With this terminology, the proton momentum is collinear and the final-state jet momentum is anti-hard-collinear. Above and in the rest of the paper we work in the reference frame where the transverse components of the external momenta vanish.

To construct the effective theory we must first identify the momentum regions that produce on-shell singularities in loop diagrams. SCET fields are then introduced to reproduce the effects of these momentum regions. The relevant momentum regions depend on the choice of x. In the kinematical regime where $1 - x \sim \Lambda_{\rm QCD}/Q$, we find that we must consider hard, anti-hard-collinear, collinear, and soft-collinear regions.

The appearance of soft-collinear instead of soft modes will have important consequences in our analysis. Before we begin, it is useful to explain their origin in simple terms. For the final-state jet to be anti-hard-collinear requires that $n_+P + n_+q = n_+p_x \sim Q\lambda^2$. This is possible only if $n_+P = -n_+q + \omega$, where ω is a residual momentum scaling as $\omega \sim Q\lambda^2$ and $-n_+q = Q$ is a large kinematic piece. This is similar to HQET, where the b-quark momentum is $m_b v + k_s$, with k_s a soft residual momentum $k_s \sim m_b(\lambda^2, \lambda^2, \lambda^2)$ and $m_b v$ a large kinematic piece. For a collinear particle, however, the residual momentum cannot be soft because $n_-k_s \sim Q\lambda^2$, while for a collinear momentum $n_-p_c \sim Q\lambda^4$. The simplest possibility is that the residual momentum scales as $Q(\lambda^2, \lambda^3, \lambda^4)$, a scaling to which we will refer as soft-collinear. We will show below that this is indeed the scaling which is relevant in loop diagrams. This leads us to interpret the soft-collinear mode as the residual momentum of a collinear field.

We will now make these observations more rigorous by analyzing a loop diagram using the method of regions [16], similarly to [15]. As a simplification, we begin with the scalar version of the triangle diagram shown in Figure 1. This allows us to identify the relevant momentum regions without complications related to Dirac algebra. The external lines carry a collinear momentum p_p and an anti-hard-collinear momentum $p_x = p_p + q$. We set all masses to zero, and regularize IR divergences by keeping the external lines off shell by an amount $p_x^2 \sim Q^2\lambda^2$ and $p_p^2 \sim P^2 \sim Q^2\lambda^4$. The integral in the full theory is given by

$$\begin{aligned} I &= \int [dL] \frac{1}{(L+p_x)^2} \frac{1}{(L+p_p)^2} \frac{1}{L^2} \\ &= \frac{1}{Q^2} \left[\ln \frac{-p_x^2}{Q^2} \ln \frac{-p_p^2}{Q^2} + \frac{\pi^2}{3} \right], \end{aligned} \tag{4}$$

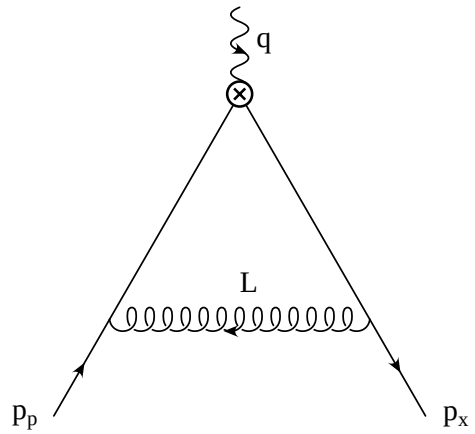

Figure 1: The triangle diagram. The momentum p_p is collinear and the momentum p_x is anti-hard-collinear.

where we have defined the measure as

$$[dL] = i16\pi^2 \left(\frac{\mu^2 e^{\gamma_E}}{4\pi}\right)^{\epsilon} \frac{d^d L}{(2\pi)^d}, \tag{5}$$

and expanded the result to leading order in λ. At leading order $Q^2 = n_+ p_p n_- p_x$.

We seek to reproduce this result by the method of regions. This strategy splits the loop integration into contributions from momentum regions according to the scaling of their light-cone components with λ. The integrand is expanded as appropriate for the particular momentum region before evaluating the integral. Once all relevant regions are identified, their sum reproduces the full theory result. We start with the hard region, where the loop momentum scales as $L \sim Q(1,1,1)$. The expanded integral is

$$\begin{aligned} I_h &= \int [dL] \frac{1}{(L^2 + n_- p_x n_+ L)} \frac{1}{(L^2 + n_+ p_p n_- L)} \frac{1}{L^2} \\ &= \frac{1}{Q^2} \left[\frac{1}{\epsilon^2} - \frac{1}{\epsilon} \ln \frac{Q^2}{\mu^2} + \frac{1}{2} \ln^2 \frac{Q^2}{\mu^2} - \frac{\pi^2}{12}\right]. \end{aligned} \tag{6}$$

We have regularized additional divergences with dimensional regularization in $d = 4 - 2\epsilon$ dimensions.

The integral I_h contains logarithms depending on the hard scale Q^2. This is a generic feature: the result for a given region always involves logarithms at that momentum scale. For this reason we need to consider the anti-hard-collinear and collinear regions, since these integrals can depend on p_x^2 and p_p^2. For the anti-hard-collinear region, where the loop momentum scales as $L \sim Q(\lambda^2, \lambda, 1)$, we find

$$\begin{aligned} I_{\bar{hc}} &= \int [dL] \frac{1}{(L + p_x)^2} \frac{1}{(n_- L n_+ p_p)} \frac{1}{L^2} \\ &= \frac{1}{Q^2} \left[-\frac{1}{\epsilon^2} + \frac{1}{\epsilon} \ln \frac{-p_x^2}{\mu^2} - \frac{1}{2} \ln^2 \frac{-p_x^2}{\mu^2} + \frac{\pi^2}{12}\right]. \end{aligned} \tag{7}$$

For the collinear region, where $L \sim Q(1, \lambda^2, \lambda^4)$, we have

$$\begin{aligned} I_c &= \int [dL] \frac{1}{(n_+ L n_- p_x)} \frac{1}{(L+p_p)^2} \frac{1}{L^2} \\ &= \frac{1}{Q^2} \left[-\frac{1}{\epsilon^2} + \frac{1}{\epsilon} \ln \frac{-p_p^2}{\mu^2} - \frac{1}{2} \ln^2 \frac{-p_p^2}{\mu^2} + \frac{\pi^2}{12} \right]. \end{aligned} \tag{8}$$

Taking the sum of the regions considered so far does not reproduce the result for the full integral (4). It is easy to check that $I - I_h - I_{\bar{hc}} - I_c$ contains logarithms depending on $p_x^2 p_p^2/Q^2 \sim Q^2 \lambda^6$. This is taken into account by including the soft-collinear region, where $L \sim Q(\lambda^2, \lambda^3, \lambda^4)$. This region gives

$$\begin{aligned} I_{sc} &= \int [dL] \frac{1}{(n_+ L n_- p_x + p_x^2)} \frac{1}{(n_- L n_+ p_p + p_p^2)} \frac{1}{L^2} \\ &= \frac{1}{Q^2} \left[\frac{1}{\epsilon^2} + \frac{1}{\epsilon} \ln \frac{Q^2 \mu^2}{p_x^2 p_p^2} + \frac{1}{2} \ln^2 \left(\frac{p_x^2 p_p^2}{Q^2 \mu^2} \right) + \frac{\pi^2}{4} \right]. \end{aligned} \tag{9}$$

Adding $I_h + I_{\bar{hc}} + I_c + I_{sc}$, we see that the poles cancel, and that we recover the result for the full integral given in (4). We will construct a version of SCET which accounts for these momentum regions in the next section.

Note that the soft and hard-collinear regions are needed in applications of SCET to B decay, but are not needed here. The soft region, where $L \sim Q(\lambda^2, \lambda^2, \lambda^2)$, is irrelevant because

$$\begin{aligned} I_s &= \int [dL] \frac{1}{(n_+ L n_- p_x + p_x^2)} \frac{1}{(n_- L n_+ p_p)} \frac{1}{L^2} \\ &= \frac{1}{Q^2} \int [dL] \frac{1}{(n_+ L + n_+ p_x)} \frac{1}{(n_- L)} \frac{1}{L^2} = 0. \end{aligned} \tag{10}$$

To derive the second line we used $p_x^2 = n_+ p_x n_- p_x$ (recall $p_{x_\perp} = 0$), and then that scaleless integrals vanish in dimensional regularization. The hard-collinear integrand, where $L \sim Q(1, \lambda, \lambda^2)$, is also scaleless and vanishes.

While it may be possible to eliminate the soft-collinear scale $\Lambda_{\rm QCD}^3/Q$ by introducing an IR regulator to cut off momentum regions with virtuality smaller than the QCD scale $\Lambda_{\rm QCD}^2$, we find it more convenient to keep the collinear quarks off shell by an amount $p_p^2 \sim P^2$ and use dimensional regularization. In our end analysis we will adopt the philosophy of [17, 18], and interpret any sensitivity of low-energy matrix elements to the soft-collinear mode as a breakdown of factorization.

We should emphasize that all results are frame independent. It is also possible to carry out the analysis in the target rest frame, where the proton momentum is soft. We can identify the scaling of the light-cone components of the momentum regions in the rest frame by performing a Lorentz boost to this frame, which amounts to rescaling $n_\pm$. The components of a generic momentum change according to $(n_+ p, p_\perp, n_- p) \to (n_+ p \lambda^2, p_\perp, n_- p \lambda^{-2})$. The correspondence between the two frames is given by

	Breit Frame		Rest Frame
hard	$Q(1,1,1)$	$\leftrightarrow$	$Q(\lambda^2,1,\frac{1}{\lambda^2})$
anti-hard-collinear	$Q(\lambda^2,\lambda,1)$	$\leftrightarrow$	$Q(\lambda^4,\lambda,\frac{1}{\lambda^2})$
collinear	$Q(1,\lambda^2,\lambda^4)$	$\leftrightarrow$	$Q(\lambda^2,\lambda^2,\lambda^2)$
soft-collinear	$Q(\lambda^2,\lambda^3,\lambda^4)$	$\leftrightarrow$	$Q(\lambda^4,\lambda^3,\lambda^2)$

Although the individual light-cone components of the momentum regions scale differently in the two frames, the number of regions is the same. Moreover, the result for each region depends on invariants at that scale and is therefore frame independent. This can be seen from the explicit results, or by noticing that each integrand is invariant under the simultaneous rescalings of $n_\pm$ shown above. In the effective theory this is referred to as reparameterization invariance (RPI) [19, 20].

3 Matching onto SCET

This section deals with matching the QCD Lagrangian and electromagnetic current onto SCET. Our eventual goal is to examine the factorization properties of the hadronic tensor using effective field theory methods. In inclusive processes all QCD effects are contained in the hadronic tensor, which is given by the spin-averaged matrix element between proton states

$$W^{\mu\nu} = \frac{1}{\pi}\mathrm{Im}\langle P|T^{\mu\nu}|P\rangle, \tag{11}$$

where the current correlator $T^{\mu\nu}$ is defined through the time-ordered product

$$T^{\mu\nu} = i\int d^4z e^{iqz}\mathrm{T}\left\{J^{\mu\dagger}(z)J^{\nu}(0)\right\}. \tag{12}$$

Here J^μ is the electromagnetic current, and q is the momentum of the incoming photon. We will evaluate the correlator in effective field theory by separating the contributions from the momentum regions identified in the previous section, namely

hard	$Q(1,1,1)$
anti-hard-collinear	$Q(\lambda^2,\lambda,1)$
collinear	$Q(1,\lambda^2,\lambda^4)$
soft-collinear	$Q(\lambda^2,\lambda^3,\lambda^4)$

We calculate the hadronic tensor using a two-step matching procedure familiar from applications of SCET to inclusive B decay in the shape-function region [3, 6, 7]. In the first step, we match the QCD Lagrangian and electromagnetic current onto SCET by integrating out fluctuations at the hard scale Q^2 and introducing effective theory

fields for the regions $p_{\bar{hc}}$, p_c, p_{sc}. The Lagrangian can be derived exactly, and will be discussed in the next sub-section. The current, on the other hand, receives corrections from fluctuations at the hard scale. These corrections can be absorbed into a hard Wilson coefficient, which we will calculate at one loop in Section 3.2. In a second step of matching we evaluate the hadronic tensor (11) using the SCET Lagrangian and current. In this step of matching we integrate out fluctuations at the hard-collinear scale $Q\Lambda_{\rm QCD}$ and match onto the parton distribution function. We discuss this at tree level in Section 4 and at one loop in Section 5.

3.1 SCET Lagrangian

The QCD Lagrangian for light quarks contains no hard scale and the SCET Lagrangian can be derived exactly [4]. For the case at hand, we have

$$\mathcal{L}_{\rm QCD} \to \mathcal{L}_{c+sc} + \mathcal{L}_{\bar{hc}+sc} + \mathcal{L}_{sc} + \mathcal{L}_{YM}, \tag{13}$$

where $\mathcal{L}_{c+sc}$ contains the collinear Lagrangian as well as interactions with the soft-collinear gluon field, and analogously for $\mathcal{L}_{\bar{hc}+sc}$. There is no interaction term $\mathcal{L}_{c+\bar{hc}}$ for processes where the initial and final states contain only one type of collinear field [18]. The soft-collinear Lagrangian $\mathcal{L}_{sc}$ can be found in [15], and the Yang-Mills Lagrangian for each sector is the same as in QCD.

The Lagrangian $\mathcal{L}_{c+sc}$ can be derived using the methods of [4, 5], as was done in [15]. The result for the leading-order Lagrangian $\mathcal{L}_{c+sc}$ is

$$\mathcal{L}_{c+sc} = \bar{\xi}_c \left(in_- D_{c+sc} + (i\not{D}_{c_\perp} - m_q) \frac{1}{in_+ D_c} (i\not{D}_{c_\perp} + m_q) \right) \frac{\not{n}_+}{2} \xi_c, \tag{14}$$

where $iD^\mu_{c+sc} = i\partial^\mu + gA^\mu_c + gA^\mu_{sc}$. In interactions between collinear and soft-collinear fields the soft-collinear fields are multipole expanded and depend on $z^\mu_- = (n_+ z) n^\mu_-/2$. We have omitted a pure glue interaction term, which will not be needed here. We can derive the Lagrangian $\mathcal{L}_{\bar{hc}+sc}$ by making the replacements $n_- \leftrightarrow n_+$ and $\phi_c \to \phi_{\bar{hc}}$ in the expressions above. The result is

$$\mathcal{L}_{\bar{hc}+sc} = \bar{\xi}_{\bar{hc}} \left(in_+ D_{\bar{hc}+sc} + i\not{D}_{\bar{hc}_\perp} \frac{1}{in_- D_{\bar{hc}}} i\not{D}_{\bar{hc}_\perp} \right) \frac{\not{n}_-}{2} \xi_{\bar{hc}}. \tag{15}$$

We have again omitted a pure glue interaction term. In interactions between anti-hard-collinear and soft-collinear fields the soft-collinear fields must be multipole expanded and depend only on $z^\mu_+ = (n_- z) n^\mu_+/2$.

We have included a collinear quark mass $m_q \sim \Lambda_{\rm QCD} \sim Q\lambda^2$ in the leading-order Lagrangian $\mathcal{L}_{c+sc}$ above. We are free to include such a mass without changing the regions analysis. In fact, keeping the collinear momentum off shell by an amount $p_p^2 \sim Q^2\lambda^4$ effectively gave such a scale to the collinear line, adding an actual mass just changes $p_p^2 \to p_p^2 - m_q^2$ in the collinear propagator. This does not eliminate soft-collinear effects. We checked this claim by modifying the scalar triangle integral to include a mass $m_q \sim$

$Q\lambda^2$ for the collinear line and confirmed that, at least to one loop, the regions analysis is unchanged. We have no proof that the regions analysis is unchanged beyond one loop, and in the following calculations we will always set $m_q = 0$ for simplicity.

A property of the Lagrangians crucial for factorization proofs is that the soft-collinear fields can be decoupled from the anti-hard-collinear and collinear fields through field redefinitions involving Wilson lines [15]. We introduce the Wilson lines

$$S_{sc}(z) = \mathrm{P}\exp\left(ig\int_{-\infty}^{0} ds\, n_- A_{sc}(z+sn_-)\right) \tag{16}$$

$$S_{\bar{sc}}(z) = \mathrm{P}\exp\left(ig\int_{-\infty}^{0} ds\, n_+ A_{sc}(z+sn_+)\right) \tag{17}$$

along with similar objects W_c and $W_{\bar{hc}}$, where the soft-collinear fields are replaced by collinear or anti-hard-collinear fields, and $n_+ \leftrightarrow n_-$. After making the field redefinitions

$$\begin{aligned} \xi_c &= S_{sc}\xi_c^{(0)}, \quad A_c = S_{sc}A_c^{(0)}S_{sc}^\dagger, \quad W_c = S_{sc}W_c^{(0)}S_{sc}^\dagger, \\ \xi_{\bar{hc}} &= S_{\bar{sc}}\xi_{\bar{hc}}^{(0)}, \quad A_{\bar{hc}} = S_{\bar{sc}}A_{\bar{hc}}^{(0)}S_{\bar{sc}}^\dagger, \quad W_{\bar{hc}} = S_{\bar{sc}}W_{\bar{hc}}^{(0)}S_{\bar{sc}}^\dagger, \end{aligned} \tag{18}$$

the fields with the superscript 0 no longer interact with the soft-collinear fields. This factorization of soft-collinear fields at the level of the Lagrangians does not guarantee the factorization of the current correlator (12), however, because the effects may reappear in time-ordered products with the external currents [17].

3.2 SCET current at one loop

Having obtained the relevant SCET Lagrangian, we now consider the one-loop matching of the electromagnetic current onto its effective field theory expression. This was done previously in [21] and we agree with the results obtained there. We will repeat the calculation to show how logarithms related to the soft-collinear mode are essential to the analysis.

At leading order the matching of the electromagnetic current onto SCET takes the form

$$\bar{\psi}_c(z)\gamma^\mu\psi_{\bar{hc}}(z) \to \int ds dt\, \tilde{C}(s,t,\mu)(\bar{\xi}_c W_c)(z+sn_+)\gamma^\mu(W_{\bar{hc}}^\dagger\xi_{\bar{hc}})(z+tn_-). \tag{19}$$

As in [21], we consider a single quark flavor with unit charge. The convolution arises because n_+p_c and $n_-p_{\bar{hc}}$ are on the order of the hard scale, so the operator can be non-local by an amount $1/Q$ in these directions. Setting z to zero and using translational invariance, the current can be written as

$$C(n_+P_c\, n_-P_{\bar{hc}},\mu)(\bar{\xi}_c W_c)(0)\gamma^\mu(W_{\bar{hc}}^\dagger\xi_{\bar{hc}})(0), \tag{20}$$

where the Fourier-transformed coefficient function is

$$C(n_+P_c\, n_-P_{\bar{hc}},\mu) = \int ds dt\, \tilde{C}(s,t)e^{i(sn_+P_c - tn_-P_{\bar{hc}})}, \tag{21}$$

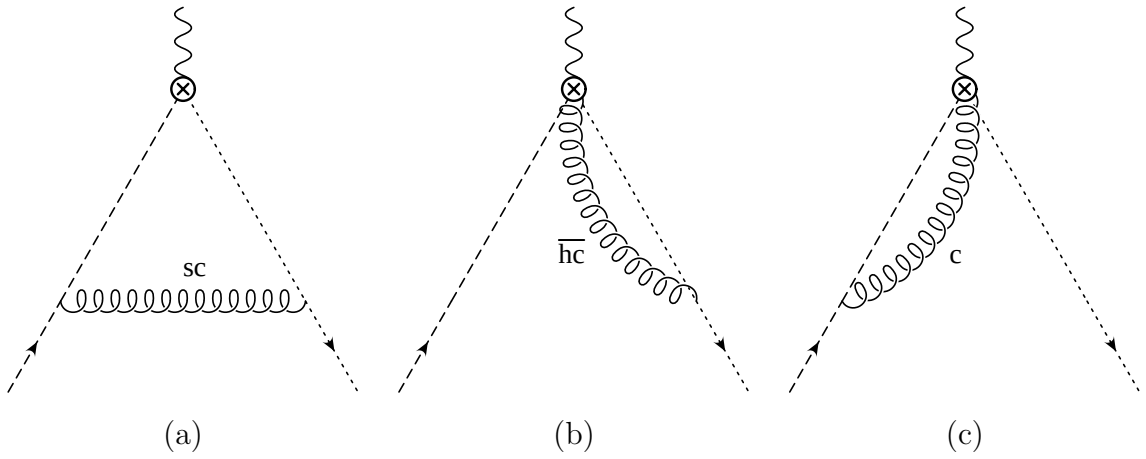

Figure 2: One-loop corrections to the SCET current. The long-dashed lines are collinear and the short-dashed lines anti-hard-collinear. The gluon scaling is indicated explicitly.

and $P_{c,\bar{hc}}$ are momentum operators. In our case these are both Q so we have $C(Q^2,\mu)$.

To calculate the one-loop matching conditions we take the difference of the QCD result from that evaluated in SCET. The QCD graph is the same as in Figure 1 but evaluated with the Feynman rules of QCD. We find it useful to break up the QCD result into contributions from each momentum region, as we did with the scalar triangle. The matching conditions are related only to the hard region. For the QCD result we find

$$\begin{aligned} I_{\rm QCD} &= \frac{C_F\alpha_s}{4\pi}\gamma^\mu\left[\frac{1}{\epsilon_{\rm UV}} - \ln\frac{Q^2}{\mu^2} - 2\ln\frac{-p_p^2}{Q^2}\ln\frac{-p_x^2}{Q^2} - 2\ln\frac{-p_p^2}{Q^2} - 2\ln\frac{-p_x^2}{Q^2} - \frac{2\pi^2}{3}\right] \\ &= I_h + I_{\bar{hc}} + I_c + I_{sc}, \end{aligned} \tag{22}$$

where

$$I_h = \frac{C_F\alpha_s}{4\pi}\gamma^\mu\left[-\frac{2}{\epsilon^2} + \frac{2}{\epsilon}\left(\ln\frac{Q^2}{\mu^2} - 2\right) + \frac{1}{\epsilon_{\rm UV}} - \ln^2\frac{Q^2}{\mu^2} + 3\ln\frac{Q^2}{\mu^2} + \frac{\pi^2}{6} - 8\right], \tag{23}$$

$$I_{\bar{hc}} = \frac{C_F\alpha_s}{4\pi}\gamma^\mu\left[\frac{2}{\epsilon^2} - \frac{2}{\epsilon}\left(\ln\frac{-p_x^2}{\mu^2} - 1\right) + \ln^2\frac{-p_x^2}{\mu^2} - 2\ln\frac{-p_x^2}{\mu^2} - \frac{\pi^2}{6} + 4\right], \tag{24}$$

$$I_c = \frac{C_F\alpha_s}{4\pi}\gamma^\mu\left[\frac{2}{\epsilon^2} - \frac{2}{\epsilon}\left(\ln\frac{-p_p^2}{\mu^2} - 1\right) + \ln^2\frac{-p_p^2}{\mu^2} - 2\ln\frac{-p_p^2}{\mu^2} - \frac{\pi^2}{6} + 4\right], \tag{25}$$

$$I_{sc} = \frac{C_F\alpha_s}{4\pi}\gamma^\mu\left[-\frac{2}{\epsilon^2} + \frac{2}{\epsilon}\ln\frac{p_x^2p_p^2}{Q^2\mu^2} - \ln^2\frac{p_x^2p_p^2}{Q^2\mu^2} - \frac{\pi^2}{2}\right]. \tag{26}$$

We have expanded all results to leading order in λ, and used that $Q^2 = n_+p_p n_-p_x$ at this order. We must supplement these graphs with the wave-function renormalization

for off-shell quarks, which gives a contribution

$$I_w = \frac{1}{2}\frac{C_F\alpha_s}{4\pi}\gamma^\mu \left[-\frac{1}{\epsilon_{\rm UV}} - 1 + \ln\frac{-p_i^2}{\mu^2}\right] \tag{27}$$

for each external quark line. The UV poles cancel in the sum $I_h + I_w$, as required by current conservation.

The next step is to evaluate the SCET diagrams in Figure 2. Evaluating the graphs in the figure using the Feynman rules of SCET reproduces the result for the QCD regions calculation. By this we mean that Figure 2(a) evaluates to I_{sc}, Figure 2(b) to $I_{\bar{hc}}$, and Figure 2(c) to I_c. This just confirms that we have constructed the effective theory correctly. The wave-function graphs in the effective theory are the same as (27) [22].

The difference between the two theories is that the hard integral I_h is absent in SCET. Its finite part is taken into account by a hard matching coefficient, and its infinite part is reproduced by a renormalization factor Z_J applied to the bare current. Including the tree-level contribution, the matching coefficient is therefore

$$C(Q^2,\mu) = 1 + \frac{C_F\alpha_s}{4\pi}\left[-\ln^2\frac{Q^2}{\mu^2} + 3\ln\frac{Q^2}{\mu^2} + \frac{\pi^2}{6} - 8\right], \tag{28}$$

and the renormalization factor is

$$Z_J = 1 + \frac{C_F\alpha_s}{4\pi}\left[-\frac{2}{\epsilon^2} - \frac{3}{\epsilon} + \frac{2}{\epsilon}\ln\frac{Q^2}{\mu^2}\right]. \tag{29}$$

The hard coefficient $C(Q^2,\mu)$ and the renormalization factor Z_J depend on the hard scale Q^2. For the infinite counter terms, this is possible only after a cancellation between logarithms that occurs when adding the anti-hard-collinear, collinear, and soft-collinear graphs. That logarithms of UV origin related to the soft-collinear field are needed to ensure that the renormalization factor Z_J depends only on the hard scale Q^2 was first noted in [17], in a slightly different context. On the other hand, no such cancellation occurs for the finite terms, where the sum of the anti-hard-collinear, collinear, and soft collinear graphs still contains logarithms at each scale. We will see in Sections 5 and 6 that the matrix element of the current correlator shares this property, and that the logarithms related to the soft-collinear scale cause problems for factorization.

4 Matching onto parton distributions at tree level

Matching onto the intermediate theory has absorbed the effects of hard fluctuations into a short-distance Wilson coefficient. This leaves the three widely separated scales $Q\Lambda_{\rm QCD} \gg \Lambda_{\rm QCD}^2 \gg \Lambda_{\rm QCD}^3/Q$. We now examine the factorization properties of the hadronic tensor (11). To achieve a perturbative factorization of the form (1), we would need to show that the soft-collinear scale $\Lambda_{\rm QCD}^3/Q$ is irrelevant. We could then perform a second and final step of matching at the scale $Q\Lambda_{\rm QCD}$, and identify the associated

matching coefficient with the jet function J. The low-energy matrix element would define a parton distribution function f characterized by fluctuations at the collinear scale $\Lambda^2_{\rm QCD}$ only, which would be linked to J in a convolution integral. The purpose of this section is to demonstrate with a tree-level example that this is impossible, by showing that soft-collinear effects do not decouple from the low-energy matrix element. In fact, the jet function is linked to the parton distribution function by a convolution variable related to the soft-collinear scale. We will argue that a full separation of scales would require integrating out the collinear scale $\Lambda^2_{\rm QCD}$ in a third step of matching, which however cannot be done perturbatively.

At leading order, the current correlator (12) is given by the time-ordered product

$$T^{\mu\nu} = i \int d^4z e^{iq\cdot z} \mathrm{T}\Big\{ \bar\chi_c(z)\gamma^\mu \chi_{\bar hc}(z) \bar\chi_{\bar hc}(0)\gamma^\nu \chi_c(0) \Big\}, \tag{30}$$

where we have defined the fields

$$\chi_c \equiv W_c^\dagger \xi_c, \qquad \chi_{\bar hc} \equiv W_{\bar hc}^\dagger \xi_{\bar hc}, \tag{31}$$

which are manifestly gauge invariant under anti-hard-collinear and collinear gauge transformations. At tree level and to lowest order in g the hard Wilson coefficient $C(Q^2,\mu)$ and the Wilson lines W are unity. We perform a second step of matching by integrating out the anti-hard-collinear fields. This is done at the scale $Q\Lambda_{\rm QCD}$, which we treat as perturbative. To do this at tree level, we first perform the decoupling redefinition (18) on the anti-hard-collinear fields (and immediately drop the superscript (0)), and then contract the anti-hard-collinear fields into a propagator. This is represented by the Feynman diagram in Figure 3(a). The anti-hard-collinear propagator is given in momentum space by

$$\langle 0|\xi_{\bar hc}(z)_{a\alpha} \bar\xi_{\bar hc}(0)_{b\beta}|0\rangle = \int \frac{d^4L}{(2\pi)^4} e^{-iLz} \frac{in_-L}{L^2+i0} \left(\frac{\bar n\!\!\!/_+}{2}\right)_{\alpha\beta} \delta_{ab}. \tag{32}$$

This forces z to scale as an anti-hard-collinear quantity, and we need to perform the multipole expansion accordingly. This is in general different from the multipole expansion in SCET Lagrangian interactions, because the photon injects a large external momentum q into the diagram. In particular, since z scales as anti-hard-collinear, the collinear and soft-collinear fields can depend only on $z_+^\mu = (n_-z/2)n_+^\mu$. The result for the current correlator is then

$$\begin{aligned} T^{\mu\nu} = &- \int d^4z e^{iqz} \bar\xi_c(z_+)\gamma^\mu S_{\bar sc}(z_+) \frac{\bar n\!\!\!/_+}{2} S_{\bar sc}^\dagger(0)\gamma^\nu \xi_c(0) \\ &\int \frac{d^4L}{(2\pi)^4} e^{-iLz} \frac{n_-L}{n_-Ln_+L + L_\perp^2 + i0} \end{aligned} \tag{33}$$

The soft-collinear and collinear fields do not depend on n_+z or $z_\perp$, so we can perform

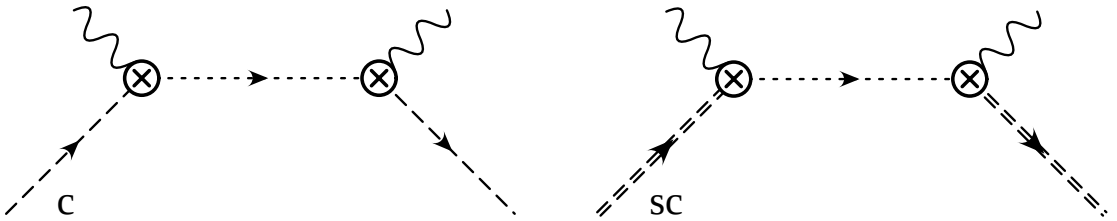

(a) (b)

Figure 3: Tree-level contribution to the current correlator in SCET, evaluated in terms of collinear fields ξ_c (a), and soft-collinear fields $\xi_{Q,sc}$ (b). The short-dashed propagator is anti-hard-collinear.

these integrations. We then have

$$T^{\mu\nu} = -\int \frac{d(n_-z)}{2}\frac{d(n_+L)}{2\pi}e^{-in_+Ln_-z/2}\frac{n_-q}{n_-qn_+L+i0}$$
$$e^{in_+qn_-z/2}\bar{\xi}_c(z_+)S_{\bar{s}c}(z_+)S^\dagger_{\bar{s}c}(0)\gamma^\mu\frac{\not{n}_+}{2}\gamma^\nu\xi_c(0). \tag{34}$$

Even though $n_+p_c \sim Q$ and $n_+p_{sc} \sim Q\lambda^2$ we cannot set the argument of the soft-collinear Wilson line $S_{\bar{s}c}(z_+)$ to zero. This is because $n_+p_c + n_+q \sim Q\lambda^2$, so we need to keep $n_+p_{sc} \sim Q\lambda^2$ in the $n_+L \sim Q\lambda^2$ component of the anti-hard-collinear propagator. We will discuss this further below. For now, we simply note that soft-collinear effects do not decouple even at leading order in the $1/Q$ expansion.

In order to calculate the hadronic tensor (11) we now take the matrix element of the current correlator between proton states. We define a parton distribution function through the spin-averaged matrix element

$$\langle P|\bar{\chi}_c(tn_+)S_{\bar{s}c}(tn_+)S^\dagger_{\bar{s}c}(0)\gamma^\mu\frac{\not{n}_+}{2}\gamma^\nu\chi_c(0)|P\rangle = \tilde{f}(t)\mathrm{tr}\left[\frac{\not{n}_-}{2}\gamma^\mu\frac{\not{n}_+}{2}\gamma_\nu\right](-n_+q). \tag{35}$$

The factor of $-n_+q = Q + \mathcal{O}(Q\lambda^2)$ preserves manifest boost invariance. Although not necessary for tree-level matching, we have reinserted the Wilson lines W_c in order to define a gauge invariant hadronic matrix element. The Fourier transformed function is

$$\tilde{f}(t) = \int d\omega e^{-i\omega t}f(\omega). \tag{36}$$

Inserting this into (33), the hadronic tensor becomes

$$W^{\mu\nu} = -\frac{1}{\pi}\mathrm{Im}\int d\omega f(\omega)\frac{Q}{n_+q-\omega+i0}\mathrm{tr}\left[\frac{\not{n}_-}{2}\gamma^\mu\frac{\not{n}_+}{2}\gamma^\nu\right]. \tag{37}$$

As written, (37) obscures the power counting in the effective theory. We have used a delta function to eliminate $n_+L \sim Q\lambda^2$, so we must have $n_+q - \omega \sim Q\lambda^2$. This requires that $\omega = n_+q + \omega_{sc}$, where $\omega_{sc} \sim Q\lambda^2$. The large component of the collinear momentum simply balances that of the incoming photon momentum, it is the residual soft-collinear component ω_{sc} which controls the dynamics. We can make this transparent by integrating out the collinear scale $\Lambda^2_{\rm QCD}$ and matching onto a low-energy theory defined at the soft-collinear scale. This is of course not possible because QCD is already strongly coupled at the collinear scale, and we will revisit this point below. At tree level, however, such a matching is trivial: we simply introduce a new field by writing $e^{iQn_-z/2}\xi_c(z) = \xi_{Q,sc}(z)$, so that $\xi_{Q,sc}$ carries the residual momentum ω_{sc}.[1] Figure 3(b) shows the tree-level diagram for the current correlator evaluated using the $\xi_{Q,sc}$. We calculate the correlator using the same steps as before, and define a distribution function f_{sc} analogously to (35), but in terms of $\xi_{Q,sc}$ instead of χ_c. We furthermore choose $n_+q = -Q + n_+p_x$, with $n_+p_x = Q(1-x)$. The result is

$$W^{\mu\nu} = \int d\omega_{sc}\, J(n_+p_x - \omega_{sc}) f_{sc}(\omega_{sc}) {\rm tr}\left[\frac{\not{n}_-}{2}\gamma^\mu\frac{\not{n}_+}{2}\gamma^\nu\right], \tag{38}$$

where

$$J(n_+p_x - \omega_{sc}) = -\frac{1}{\pi}{\rm Im}\frac{Q}{n_+p_x - \omega_{sc} + i0} = Q\delta(n_+p_x - \omega_{sc}). \tag{39}$$

This completes the tree-level matching calculation. We could have obtained this same result in the free-quark decay picture by calculating the diagram in Figure 3 and taking the imaginary part. In the free-quark picture at tree level we can interpret $f_{sc}(\omega_{sc}) = \delta(\omega_{sc})$, so that the convolution $J \otimes f_{sc}$ reproduces the result for the diagram. We went through the extra step of defining the parton distribution function in terms of a hadronic matrix element in order to draw some parallels between (38) and the factorization formula derived for inclusive B decay in the shape-function region, where one finds a convolution of the form [1, 3]

$$\int d\omega_s\, J(n_+p_x - \omega_s) S(\omega_s), \tag{40}$$

with $n_+p_x = m_b(1-x) \sim \Lambda_{\rm QCD}$. The function $J(\omega_s)$ is a perturbatively calculable jet function containing physics at the scale $m_b\Lambda_{\rm QCD}$, and $S(\omega_s)$ is a shape function containing non-perturbative effects at the scale $\Lambda^2_{\rm QCD}$. It is defined by the HQET matrix element

$$S(\omega_s) = \int dt e^{-it\omega_s}\langle \bar{B}_v|\bar{h}_v(tn_-)\, h_v(0)|\bar{B}_v\rangle. \tag{41}$$

The crucial difference between B decay and DIS is that the heavy-quark field h_v carries a residual momentum ω_s which is soft. Matching can be stopped at the perturbative scale $m_b\Lambda_{\rm QCD}$. This should be compared with (38), where the convolution involves the soft-collinear residual momentum ω_{sc}. To isolate the physics at this low scale requires

[1] This field is similar to the SCET field $\xi_{Q,n}$ defined in the label formalism [3], the difference being that the residual momentum is soft-collinear instead of ultra-soft.

an extra step of matching at the scale $p_p^2 \sim \Lambda_{\rm QCD}^2$. We did this above in order to define f_{sc}, but it is important to understand that this was only a formal manipulation. Since we cannot do this matching perturbatively, we must always lump the collinear and soft-collinear effects together into one non-perturbative function. We will emphasize in Section 6 that any sensitivity of the parton distribution function to the soft-collinear scale signals a breakdown of factorization. However, to explain how effective field theory could in principle be used to separate all the scales, we end this section by considering a fictitious QCD where perturbation theory is valid at the collinear scale. In this fictitious theory we can remove collinear fluctuations when matching the electromagnetic current onto SCET. This matching takes the form

$$\bar{\psi}_c \gamma^\mu \psi_{\bar{hc}} \to C(Q^2,\mu) D_c(p_p^2,\mu) \bar{\xi}_{Q,sc} \gamma^\mu \chi_{\bar{hc}}. \tag{42}$$

The matching coefficient $D_c(p_p^2,\mu)$ reproduces the effects of collinear loop diagrams, and could be obtained at one loop from the finite part of our expressions in Section 3.2, see (23-26). To consider such a (fictitious) matching of the SCET current will be useful in some of the discussion in the next two sections.

5 Matching onto parton distributions at one loop

In this section we examine the one-loop corrections to the current correlator (12), and interpret the results in terms of the effective theory. The relevant one-loop diagrams are shown in Figure 4. Note that the graph in Figure 4(e) containing collinear exchange, as well as graphs 4(h) and 4(i), are not actually SCET graphs. In these graphs the short-dashed propagator is hard, not anti-hard-collinear. It was our intention to remove all hard fluctuations in the first step of matching, but we have clearly not done so. Although these graphs are power suppressed by a factor of $p_x^2/Q^2 \sim \lambda^2$, we find it awkward to generate power-suppressed graphs from the leading-order Feynman rules of the effective theory. A formal solution to this problem is to remove the collinear scale when matching the current, as in (42). We cannot do this matching perturbatively, but we are interested only in the sum of collinear and soft-collinear graphs, which can equally well be written in this way. This simplifies the book-keeping, because after taking this step the graphs 4(e), 4(h) and 4(i) no longer exist, so the short-dashed propagator is always anti-hard-collinear. Note that we have not drawn box diagrams related to gluon distributions. These are power suppressed, either because the intermediate propagator is hard, analogously to 4(h), or because they involve insertions of soft-collinear quark fields (not to be confused with $\xi_{Q,sc}$), which are absent from the leading order SCET Lagrangian [15].

We now give results for the remaining diagrams, which we calculate using the free-quark picture. As before, we keep the external collinear quarks off shell by an amount p_p^2 when performing the matching. We work in Feynman gauge. With this choice of gauge graphs 4(d) and 4(e) vanish, as do the parts of 4(b), 4(f) involving soft-collinear exchange, since $n_\pm^2 = 0$. We suppress the Dirac structure, which is always the same as in

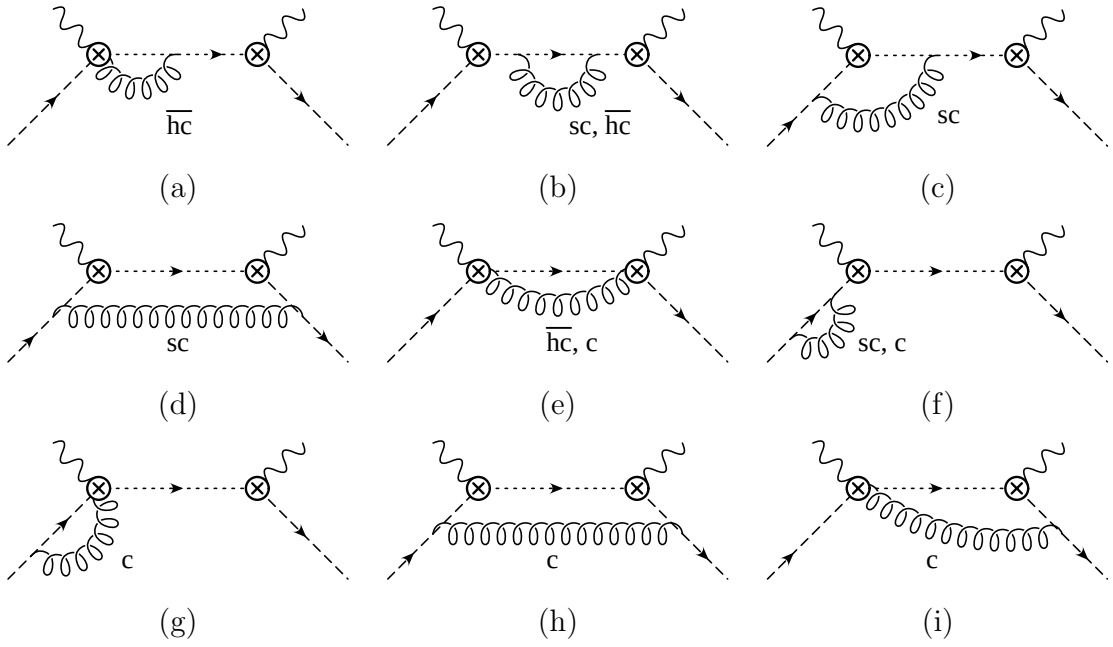

Figure 4: One-loop corrections to the current correlator. The long-dashed lines are collinear and the short-dashed lines anti-hard-collinear. The gluon scaling is labeled explicitly. The mirror image graphs are not shown. The part of (e) involving collinear exchange, (h), and (i) should *not* be included in the effective theory.

the tree-level expression (35) after summing over spins, and also the Wilson coefficients $C^2(Q^2,\mu)$, which appear as a multiplicative factor.

The non-vanishing anti-hard-collinear graphs add up to

$$T_{\bar{hc}} = -\frac{C_F\alpha_s}{4\pi}\frac{Q^2}{p_x^2}\left\{\left[-\frac{1}{\epsilon}-1+\ln\frac{-p_x^2}{\mu^2}\right]\right.$$
$$\left.+\left[\frac{4}{\epsilon^2}+\frac{4}{\epsilon}\left(1-\ln\frac{-p_x^2}{\mu^2}\right)+2\ln^2\frac{-p_x^2}{\mu^2}-4\ln\frac{-p_x^2}{\mu^2}-\frac{\pi^2}{3}+8\right]\right\}, \tag{43}$$

the collinear graphs (including wave-function graphs) evaluate to

$$T_c = -\frac{C_F\alpha_s}{4\pi}\frac{Q^2}{p_x^2}\left\{\left[-\frac{1}{\epsilon}-1+\ln\frac{-p_p^2}{\mu^2}\right]\right.$$
$$\left.+\left[\frac{4}{\epsilon^2}+\frac{4}{\epsilon}\left(1-\ln\frac{-p_p^2}{\mu^2}\right)+2\ln^2\frac{-p_p^2}{\mu^2}-4\ln\frac{-p_p^2}{\mu^2}-\frac{\pi^2}{3}+8\right]\right\}, \tag{44}$$

and the soft-collinear graphs give

$$T_{sc} = -\frac{C_F\alpha_s}{4\pi}\frac{Q^2}{p_x^2}\left[-\frac{4}{\epsilon^2}+\frac{4}{\epsilon}\ln\frac{p_x^2p_p^2}{Q^2\mu^2}-2\ln^2\frac{p_x^2p_p^2}{Q^2\mu^2}-\pi^2\right]. \tag{45}$$

The $1/\epsilon$ terms in the sum of all diagrams is subtracted by the current renormalization factor Z_J^2 given in (29). This is possible only after the same cancellation between logarithms in the divergent pieces of the anti-hard-collinear, collinear, and soft-collinear graphs that we observed when matching the SCET current. No such cancellation occurs in the finite pieces, where logarithms at each scale remain. We can interpret the finite parts as the one-loop corrections to a convolution of functions characterizing the physics at the various scales. This takes the form

$$\frac{1}{\pi}\mathrm{Im}\left(T_{\bar{hc}}+T_c+T_{sc}\right) = J^{(1)}\otimes\left[S^{(0)}\cdot f_{sc}^{(0)}\right]+J^{(0)}\otimes\left[S^{(1)}\cdot f_{sc}^{(0)}+S^{(0)}\cdot f_{sc}^{(1)}\right]. \tag{46}$$

The superscript refers to the n-loop correction to each function. We have defined a function $S = D_c^2$ (see (42)), which takes into account collinear effects, and grouped the sum of the collinear and soft-collinear corrections inside the square brackets. In this step of matching we want to obtain the one-loop correction to the jet function J. To do this rigorously, we would first need to calculate the renormalized expression for the object $[S\cdot f_{sc}]$, using the free-quark picture. This calculation would require a more precise formulation of an effective theory defined at the soft-collinear scale. We will not go through this exercise here, but rather assume that we can construct a low-energy theory that properly accounts for the IR physics related to the collinear and soft-collinear fields. The difference between this low-energy theory and SCET is that the anti-hard-collinear fields are absent, so the the matching function J is given by imaginary part of the finite piece of $T_{\bar{hc}}$ in (43). This imaginary part is singular at $p_x^2=0$ and must be interpreted in terms of distributions to be integrated against a smooth function $F(p_x^2)$. To stay in the region where the SCET treatment is valid requires a cut on p_x^2, so we find it convenient to express the results in terms of star distributions, which are defined as [23]

$$\begin{aligned}\int_{\le 0}^{z} dx F(x)\left(\frac{1}{x}\right)_*^{[u]} &= \int_0^z dx\frac{F(x)-F(0)}{x}+F(0)\ln\frac{z}{u},\\ \int_{\le 0}^{z} dx F(x)\left(\frac{\ln(x/u)}{x}\right)_*^{[u]} &= \int_0^z dx\frac{F(x)-F(0)}{x}\ln\frac{z}{u}+\frac{F(0)}{2}\ln^2\frac{z}{u}.\end{aligned} \tag{47}$$

In terms of these distributions, we find

$$\begin{aligned}J^{(1)}\otimes\left[S^{(0)}\cdot f_{sc}^{(0)}\right] &= \frac{1}{\pi}\mathrm{Im}\,T_{\bar{hc}}\\ &= Q^2\frac{C_F\alpha_s}{4\pi}\left[\left(7-\pi^2\right)\delta(p_x^2)-3\left(\frac{1}{p_x^2}\right)_*^{[\mu^2]}+4\left(\frac{\ln(p_x^2/\mu^2)}{p_x^2}\right)_*^{[\mu^2]}\right].\end{aligned} \tag{48}$$

In the limit $x \to 1$ the star distribution is related to the plus distribution, and (48) agrees with a corresponding expression in [21]. This matching function also appears in inclusive B decay in the shape-function region [6, 7].

Having obtained an expression for the one-loop jet function, we end this section by taking a closer look at the low-energy physics relevant to the parton distribution function. If the hadronic tensor obeyed the factorization formula (1), then the low-energy physics would depend on the collinear scale $\Lambda^2_{\rm QCD}$ only. However, we have shown that the low-energy theory contains a product of collinear and soft-collinear functions, what we called $[S \cdot f_{sc}]$ above, and that this object contains logarithms at both the collinear and soft-collinear scales. The soft-collinear scale $\Lambda^3_{\rm QCD}/Q$ depends on the large energy Q, so not all of the Q dependence has been factorized into the hard coefficient $C(Q^2, \mu)$. We will explain the consequences of this in the next section.

6 Soft-collinear effects and factorization

In this section we consolidate our results concerning the factorization of the hadronic tensor. To summarize, we found that for values of x satisfying $1 - x \sim \Lambda_{\rm QCD}/Q$, DIS involves four scales

$$Q^2 \gg Q\Lambda_{\rm QCD} \gg \Lambda^2_{\rm QCD} \gg \Lambda^3_{\rm QCD}/Q. \tag{49}$$

The relevance of the soft-collinear scale $\Lambda^3_{\rm QCD}/Q$ makes it impossible to derive a factorization formula of the type (1). To clarify this, we find it useful to first consider a fictitious version of QCD, where the collinear scale $\Lambda^2_{\rm QCD}$ is perturbative and the soft-collinear scale is non-perturbative. In this fictitious QCD, we can derive a factorization formula by matching onto a low-energy theory defined at the soft-collinear scale. To do so, we split up the initial-state parton momentum as $p_p = Qn_-/2 + p_{sc}$, where the soft-collinear residual momentum satisfies $n_+p_{sc} \sim Q(1-x) \sim \Lambda_{\rm QCD}$ and $n_-p_{sc} \sim M_P^2/Q \sim \Lambda^2_{\rm QCD}/Q$. This treats the parton as a massless on-shell collinear quark carrying momentum $Qn_-/2$, which receives a residual momentum p_{sc} through interactions with soft-collinear partons. Beyond tree level the factorization formula contains a convolution between f_{sc} and D_c, in addition to that between f_{sc} and J. This is because $n_-p_{sc} \sim n_-p_c$, so the n_-p_{sc} momentum can be distributed between the collinear and soft-collinear fields, just as the $n_+p_{sc} \sim n_+p_x$ momentum can be distributed between the anti-hard-collinear and soft-collinear fields. Writing the mass scales (49) in terms of Q, p_{sc}, and p_x we find a factorization formula of the form

$$W \sim H\left(\frac{Q^2}{\mu^2}\right) J\left(\frac{Qn_+p_x - Qn_+p_{sc}}{\mu^2}\right) \otimes f_{sc}\left(\frac{n_-p_{sc}n_+p_{sc}}{\mu^2}\right) \otimes S\left(\frac{Qn_-p_{sc}}{\mu^2}\right), \tag{50}$$

where n_+p_{sc} and n_-p_{sc} are convolution variables. The hard function H and the soft function S are related to the Wilson coefficients arising when matching the SCET current as in (42), $H = C^2$ and $S = D_c^2$. The jet function J is calculated as explained in Section 5, and the soft-collinear function f_{sc} is defined by the spin-averaged matrix element in (35), but with $\chi_c \to \xi_{Q,sc}$. The jet function J and the collinear function S

are not linked directly through a convolution. Instead, they are linked to each other only through a mutual convolution with the function f_{sc}. Although this formula is qualitatively different from (1), we could in principle derive the renormalization group equations for this effective theory, and use them to resum all large logarithms involving the ratio $\Lambda_{\rm QCD}/Q$. This scenario has been mentioned in [17], in analogy with techniques used for the off-shell Sudakov form factor [24, 25].

Our derivation of (50) was based on an effective field theory approach that integrated out the larger scales until reaching the smallest scale, which is soft-collinear. In real QCD it is not possible to use perturbation theory at the scale $\Lambda^2_{\rm QCD}$. This obligates us to stop the matching procedure at the jet scale $Q\Lambda_{\rm QCD}$ and lump the collinear and soft-collinear effects into one non-perturbative function. We have seen that some cancellations occur between the sum of the infinite parts of the collinear and soft-collinear graphs, but this does not occur in the finite pieces defining the matrix elements. The hadronic tensor therefore takes the form

$$W \sim H\left(\frac{Q^2}{\mu^2}\right) J\left(\frac{Qn_+p_x - Qn_+p_{sc}}{\mu^2}\right) \otimes f\left(\frac{\Lambda^2_{\rm QCD}}{\mu^2}, \frac{\Lambda^2_{\rm QCD} n_+p_{sc}}{Q\mu^2}\right), \tag{51}$$

where we have inserted the physical scaling $n_-p_{sc} \sim \Lambda^2_{\rm QCD}/Q$. The notation makes clear that the parton distribution function f contains physics at both the collinear and soft-collinear scales. We cannot match perturbatively at the scale $\Lambda^2_{\rm QCD}$, so we have no way of deriving a low-energy theory that would allow us to resum logarithms at the soft-collinear scale, and large logarithms depending on $\Lambda_{\rm QCD}/Q$ remain. In other words, the parton distribution function contains a non-perturbative dependence on the large energy Q. This is different from both (1) and (50). We conclude that a perturbative factorization of scales is not possible in this region of phase space.

7 Comparison with previous work

7.1 Diagrammatic Approach

Factorization formulas for deep inelastic scattering near the endpoint have been derived using diagrammatic methods in [26, 27, 28]. It seems that the effective field theory calculation leads us to different conclusions concerning the perturbative factorization of scales. The differences can be traced directly to the soft-collinear mode. In turn, we found that the soft-collinear mode is relevant in a very specific region of phase space, where $1-x$ is correlated with $\Lambda_{\rm QCD}/Q$ through the relation $1-x \sim \Lambda_{\rm QCD}/Q \sim \lambda^2$. To the best of our knowledge, such a power counting has not been implemented within the diagrammatic approach, where one takes the limit $1-x \to 0$ without making the above-mentioned correlation. To understand the significance of this, recall that the effective field theory approach led us to split the parton distribution function into two parts according to

$$f \to S\left(\frac{Qn_-p_{sc}}{\mu^2}\right) f\left(\frac{n_-p_{sc}n_+p_{sc}}{\mu^2}\right) \sim S\left(\frac{\Lambda^2_{\rm QCD}}{\mu^2}\right) f\left(\frac{\Lambda^2_{\rm QCD}(1-x)}{\mu^2}\right). \tag{52}$$

A very similar observation has been made in the diagrammatic approach, where S and f are related to ϕ and V [26]. The function f is linked to the jet function J by the convolution variable n_+p_{sc}. Boost invariance and dimensional analysis require that this enter the parton distribution function in the combination $n_-p_{sc}n_+p_{sc}/\mu^2$. From this alone it is apparent that the parton distribution function involves fluctuations at two scales, as shown above. The second scale depends on $1-x$, and need not be soft-collinear. One sees this clearly from (9). For generic values of $p_x^2 \approx Q^2(1-x)$, the soft-collinear region is replaced by an x-dependent soft region scaling as $(Q(1-x), \Lambda_{\rm QCD}\sqrt{(1-x)}, \Lambda^2_{\rm QCD}/Q)$. The function f is associated with the vacuum matrix element of a Wilson loop built out of gauge fields with this scaling. As long as $n_+p_{sc} \sim Q(1-x) \sim Q\lambda_D$, with λ_D numerically small but still $\mathcal{O}(1)$, then both the collinear modes and these additional soft modes are parametrically of the order $\Lambda^2_{\rm QCD}$. Formulas derived with the diagrammatic approach are valid within this particular large-x limit. We emphasize that this is a different large-x limit than that considered in our work. The non-factorizable soft-collinear effects studied here emerge for values of x satisfying $1-x \sim \Lambda_{\rm QCD}/Q$. To apply effective field theory methods in the most straightforward way requires that we make this correlation, because only then can we calculate the results as an expansion in a single small parameter λ. This power counting for $1-x$ also ensures that we avoid the resonance region, where $1-x \sim \Lambda^2_{\rm QCD}/Q^2$. The failure of factorization for $1-x \sim \Lambda_{\rm QCD}/Q$ suggests that the most useful application of SCET to DIS in the endpoint region might instead use a multi-scale approach to study the limit $1-x \to \Lambda_{\rm QCD}/Q$ more carefully. This would involve replacing the soft-collinear modes by the x-dependent soft modes identified above, carefully re-deriving the factorization formula for the large-x limit obtained within the diagrammatic approach [26], and studying power corrections in terms of SCET operators. This could make use of techniques similar to those developed for the multi-scale operator expansion in inclusive B decay [29].

7.2 SCET based approach

The first application of SCET to DIS can be found in [30], which is however limited to the standard OPE region and has little overlap with our work. In [21] Manohar carried out a SCET analysis of DIS at large x, also using a two-step matching procedure. In the first step, the author matched QCD in the Breit frame onto a version of SCET involving hard-collinear fields interacting with anti-hard-collinear fields via soft gluon exchange. This differs from the version of SCET used here, which involves collinear fields interacting with anti-hard-collinear fields via soft-collinear gluon exchange. While our two approaches differ conceptually, our results for the anomalous dimension and hard matching coefficient of the SCET current agree. The results are the same because the leading-order Lagrangians $\mathcal{L}_{c+sc}$, $\mathcal{L}_{\bar{hc}+sc}$ are of the same form as $\mathcal{L}_{hc+s}$, $\mathcal{L}_{\bar{hc}+s}$. The author used these results to derive some interesting consequences for the anomalous dimension of the SCET current. We disagree on some points concerning the calculation of the hadronic tensor in the second step of matching. The major difference is that [21] found that the effects of soft gluon exchange are irrelevant to the low-energy matrix element

defining the parton distribution function (in the Breit frame). Using the translation between the leading-order Lagrangians given above, this would imply the irrelevance of soft-collinear effects, which we did not observe here. This also contradicts the results for the large-x limit derived in the diagrammatic approach, where the low-energy matrix element splits into a product of collinear and soft functions, often called ϕ and V [26].

8 Conclusions

We used soft-collinear effective theory to examine the factorization properties of deep inelastic scattering in the region of phase space where $1-x \sim \Lambda_{\rm QCD}/Q$. An analysis of loop diagrams in the Breit frame showed that the appropriate effective theory includes anti-hard-collinear, collinear, and soft-collinear fields. We found that soft-collinear effects ruin perturbative factorization. An attempt to use SCET to prove a perturbative factorization formula yields instead an expression where the low-energy matrix element defining the parton distribution function contains a non-perturbative dependence on the large energy Q. It is therefore impossible to separate the three scales $Q^2 \gg Q\Lambda_{\rm QCD} \gg \Lambda_{\rm QCD}^2$ in terms of a factorization formula. These complications related to the soft-collinear mode are similar to those found in a SCET analysis of the heavy-to-light form factors relevant to exclusive B meson decay [14]. They do not appear in an analysis of factorization for inclusive B decay in the shape-function region, where the presence of a heavy quark ensures that soft instead of soft-collinear fields are relevant to the effective theory construction.

Our conclusions are true as long as $1-x$ is correlated with $\Lambda_{\rm QCD}/Q$ through the relation $1-x \sim \Lambda_{\rm QCD}/Q$. If $1-x$ is numerically small but still larger than $\Lambda_{\rm QCD}/Q$, the standard large-x factorization formula derived within the diagrammatic approach is valid. As $1-x$ approaches the endpoint, however, non-factorizable soft-collinear effects emerge. It would be interesting to use a multi-scale effective field theory approach to carefully re-derive the large-x factorization formula using SCET, quantify power corrections in terms of SCET operators, and more carefully study the limit $1-x \to \Lambda_{\rm QCD}/Q$.

Acknowledgements

I am grateful to Thomas Becher, Thorsten Feldmann, Thomas Mannel, and Matthias Neubert for useful discussions and comments on the manuscript. This work was supported by the DFG Sonderforschungsbereich SFB/TR09 "Computational Theoretical Particle Physics".

References

[1] G. P. Korchemsky and G. Sterman, Phys. Lett. B **340** (1994) 96 [hep-ph/9407344].

[2] C. W. Bauer, S. Fleming, D. Pirjol and I. W. Stewart, Phys. Rev. D **63** (2001) 114020 [hep-ph/0011336].

[3] C. W. Bauer, D. Pirjol and I. W. Stewart, Phys. Rev. D **65**, 054022 (2002) [hep-ph/0109045].

[4] M. Beneke, A. P. Chapovsky, M. Diehl and T. Feldmann, Nucl. Phys. B **643**, 431 (2002) [hep-ph/0206152].

[5] M. Beneke and T. Feldmann, Phys. Lett. B **553**, 267 (2003) [hep-ph/0211358].

[6] C. W. Bauer and A. V. Manohar, Phys. Rev. D **70**, 034024 (2004) [hep-ph/0312109].

[7] S. W. Bosch, B. O. Lange, M. Neubert and G. Paz, Nucl. Phys. B **699**, 335 (2004) [hep-ph/0402094].

[8] K. S. M. Lee and I. W. Stewart, [hep-ph/0409045].

[9] S. W. Bosch, M. Neubert and G. Paz, JHEP **0411**, 073 (2004) [hep-ph/0409115].

[10] M. Beneke, F. Campanario, T. Mannel and B. D. Pecjak, [hep-ph/0411395].

[11] R. J. Hill and M. Neubert, Nucl. Phys. B **657**, 229 (2003) [hep-ph/0211018].

[12] C. W. Bauer, D. Pirjol and I. W. Stewart, Phys. Rev. D **67**, 071502 (2003) [hep-ph/0211069].

[13] M. Beneke and T. Feldmann, Nucl. Phys. B **685**, 249 (2004) [hep-ph/0311335].

[14] B. O. Lange and M. Neubert, Nucl. Phys. B **690**, 249 (2004) [hep-ph/0311345].

[15] T. Becher, R. J. Hill and M. Neubert, Phys. Rev. D **69**, 054017 (2004) [hep-ph/0308122].

[16] M. Beneke and V. A. Smirnov, Nucl. Phys. B **522** (1998) 321 [hep-ph/9711391].

[17] T. Becher, R. J. Hill, B. O. Lange and M. Neubert, Phys. Rev. D **69** (2004) 034013 [hep-ph/0309227].

[18] T. Becher, R. J. Hill and M. Neubert, [hep-ph/0503263].

[19] A. V. Manohar, T. Mehen, D. Pirjol and I. W. Stewart, Phys. Lett. B **539** (2002) 59 [hep-ph/0204229].

[20] J. Chay and C. Kim, Phys. Rev. D **65** (2002) 114016 [hep-ph/0201197].

[21] A. V. Manohar, Phys. Rev. D **68** (2003) 114019 [hep-ph/0309176].

[22] C. W. Bauer, S. Fleming and M. E. Luke, Phys. Rev. D **63** (2001) 014006 [hep-ph/0005275].

[23] F. De Fazio and M. Neubert, JHEP **9906**, 017 (1999) [hep-ph/9905351].

[24] G. P. Korchemsky, Phys. Lett. B **220** (1989) 629.

[25] J. H. Kuhn, A. A. Penin and V. A. Smirnov, Eur. Phys. J. C **17** (2000) 97 [hep-ph/9912503].

[26] G. Sterman, Nucl. Phys. B **281**, 310 (1987).

[27] S. Catani and L. Trentadue, Nucl. Phys. B **327** (1989) 323.

[28] G. P. Korchemsky and G. Marchesini, Nucl. Phys. B **406** (1993) 225 [hep-ph/9210281].

[29] M. Neubert, Eur. Phys. J. C **40** (2005) 165 [hep-ph/0408179].

[30] C. W. Bauer, S. Fleming, D. Pirjol, I. Z. Rothstein and I. W. Stewart, Phys. Rev. D **66** (2002) 014017 [hep-ph/0202088].